

Supporting Information

Dual mode selective chemosensor for copper and fluoride ions: A fluorimetric, colorimetric and theoretical investigation

Soumen Ghosh^a, Aniruddha Ganguly^a, Md. Raihan Uddin^b, Sukhendu Mandal^b, Md. Akhtarul Alam^{c*}, and Nikhil Guchhait^{a*}

^aDepartment of Chemistry

University of Calcutta

92, A.P.C. Road, Kolkata 700 009, India

Telephone 91-33-23508386

Fax: 91-33-23519755

^bDepartment of Microbiology

University of Calcutta

35, B. C. Road, Ballygunge

Kolkata- 700019

^cDepartment of Chemistry

Aliah University

IIA/27, New Town, Kolkata-700 156, West Bengal, India

*Corresponding author, E-mail: alam_iitg@yahoo.com (M. A. A.)

and

nguchhait@yahoo.com (N.G.)

Table of Contents

1. Characterization.....	S4
2. X-ray Crystallographic Structures.....	S6
3. UV-vis Spectra.....	S9
4. Emission spectra.....	S10
5. Theoretically optimized structure	S15
6. UV-vis Spectral data of 1 with F ⁻	S16
7. ¹ H NMR titration	S17

1. Characterization:

1.1 ^1H NMR Spectra

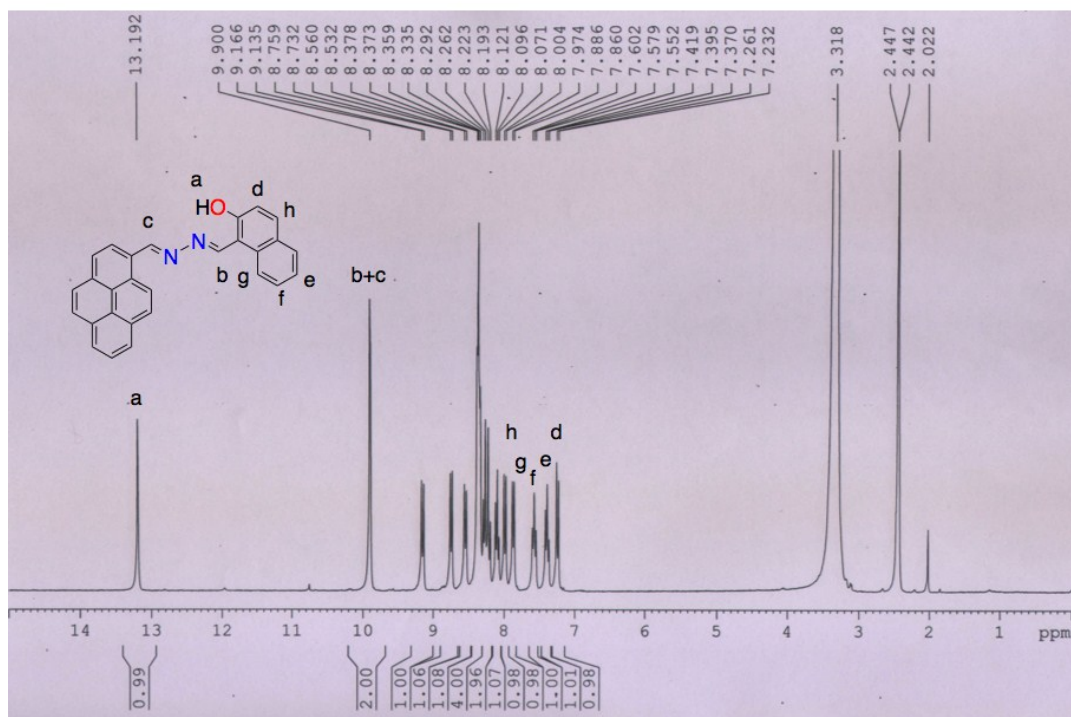


Fig. S1. ^1H NMR (300 MHz) spectrum of **1** in d_6 -DMSO at 20 °C

1.2 Mass (TOF-MS ES+) Spectra

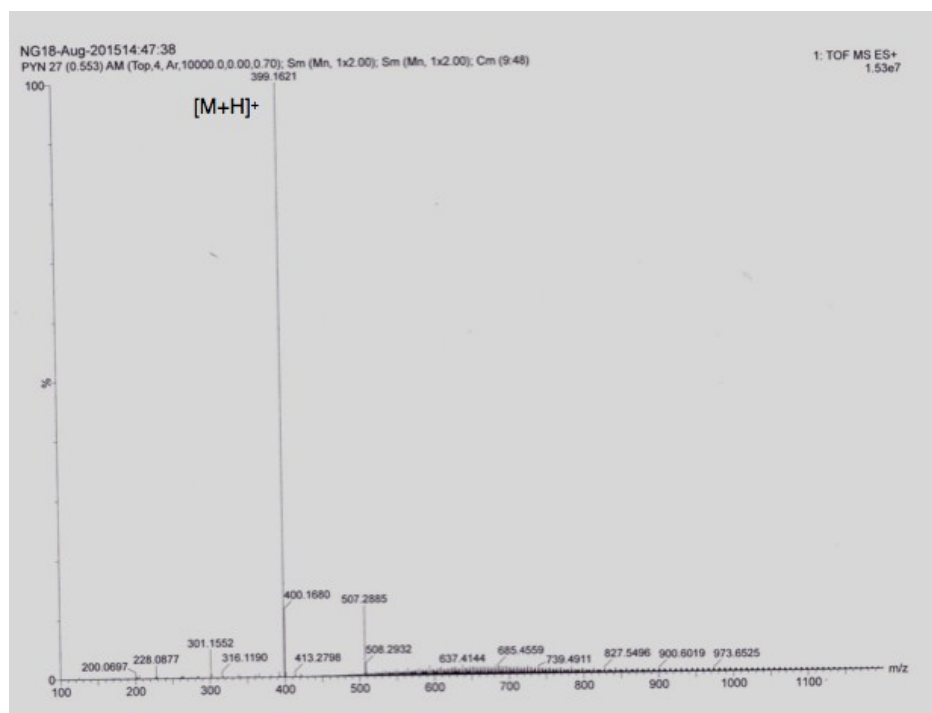


Fig. S2. Mass spectra (TOF-MS ES+) of **1**

2. X-ray Crystallographic Structures

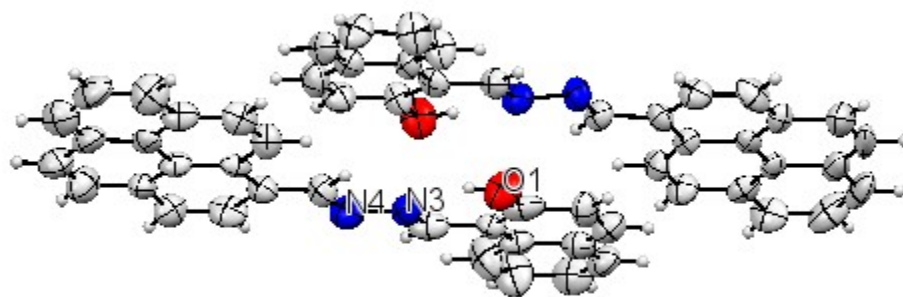


Fig. S3 ORTEP diagram of **1** (thermal ellipsoids set to 30% probability).

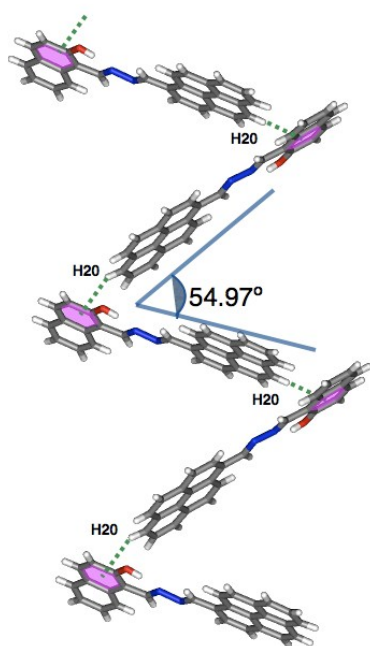


Fig. S4 1D polymer through CH... π interaction

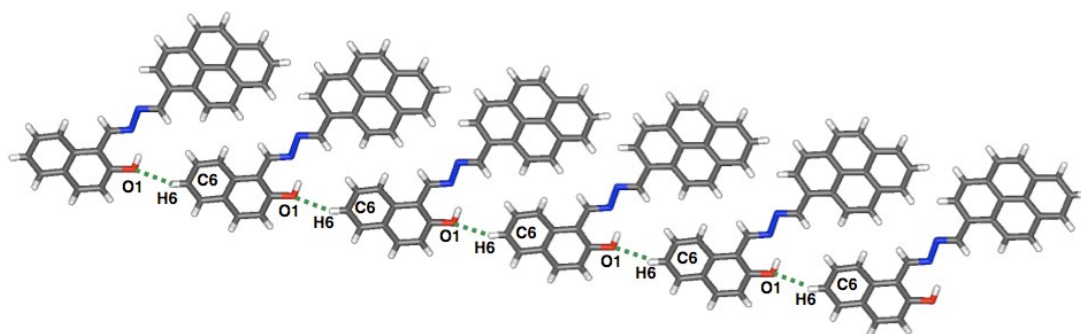


Fig. S5 1D polymer through intermolecular H-bonding interaction

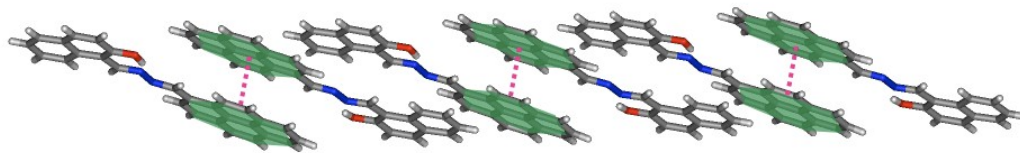


Fig. S6 Different type of $\pi \dots \pi$ interaction

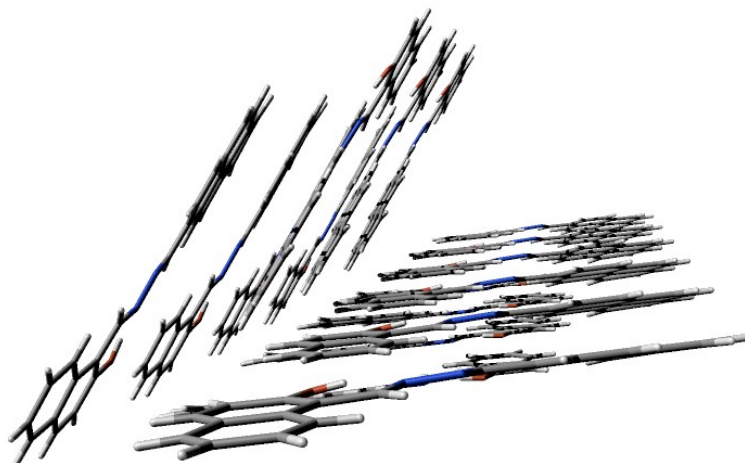


Fig. S7 2D polymeric structure of **1**

3. UV-Vis Spectra

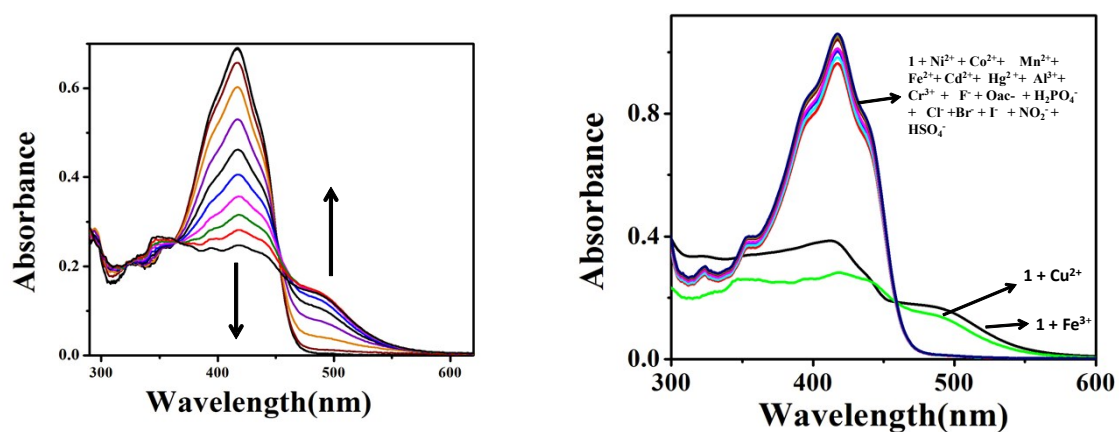


Fig. S8 UV-vis spectral changes of **1** (1.0×10^{-6} M) upon addition of (0–2 equiv.) Cu (ClO₄)₂ in methanol water mixture (7:3, v/v) (left) and UV-vis spectral changes of sensor **1** (1×10^{-6} M) in presence of various metal ions and anions (2 equiv.) in methanol water mixture (7:3, v/v) (right).

4. Emission Spectra

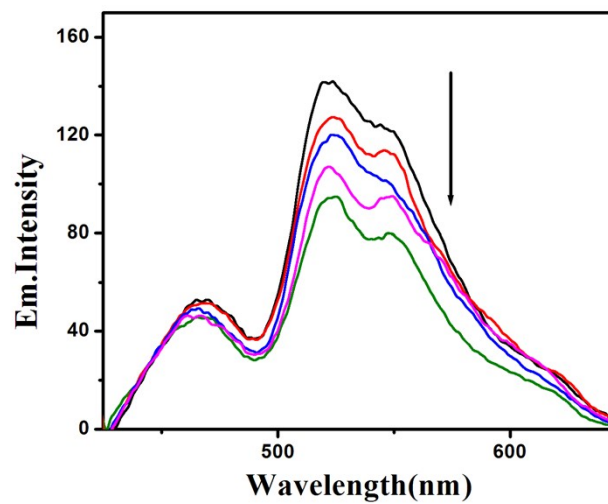


Fig. S9 Emission spectral changes of Sensor **1** (1×10^{-7} M) with dilution in methanol water mixture (7:3, v/v).

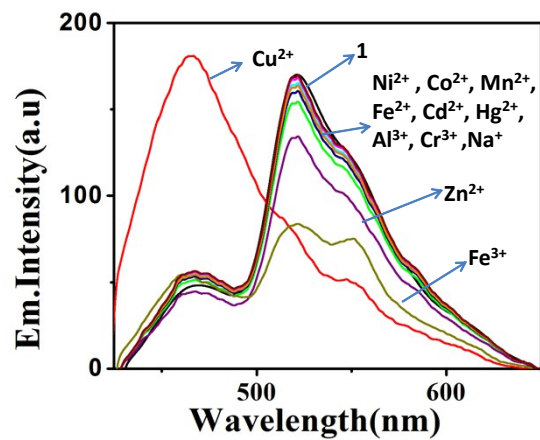


Fig. S10 Emission spectral changes of sensor **1**(1×10^{-7} M) in presence of various metal ions (2 equiv.) in methanol water mixture (7:3, v/v)

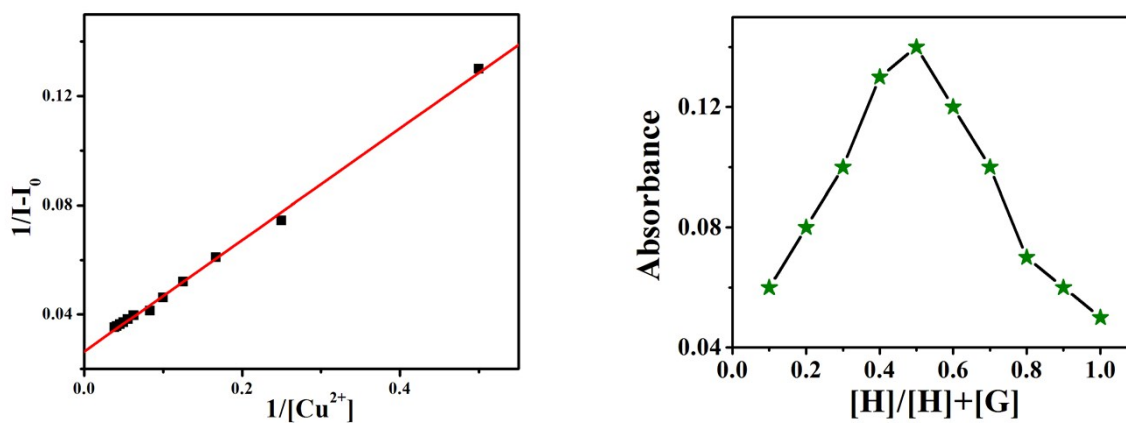


Fig. S11 B-H plot from fluorescence titration spectra at 466 nm (left) and Job's plot from Uv-vis titration at 490 nm (right) of receptor **1** with Cu^{2+} showing 1:1 binding stoichiometry.

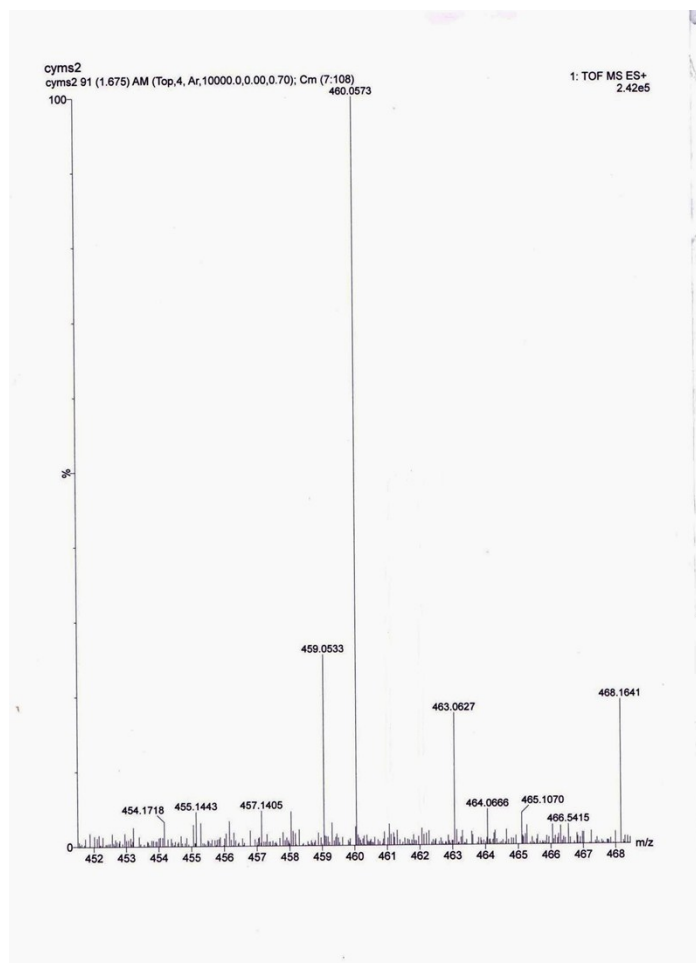


Fig. S12 Mass spectra (TOF-MS ES+) of **1-Cu²⁺** complex

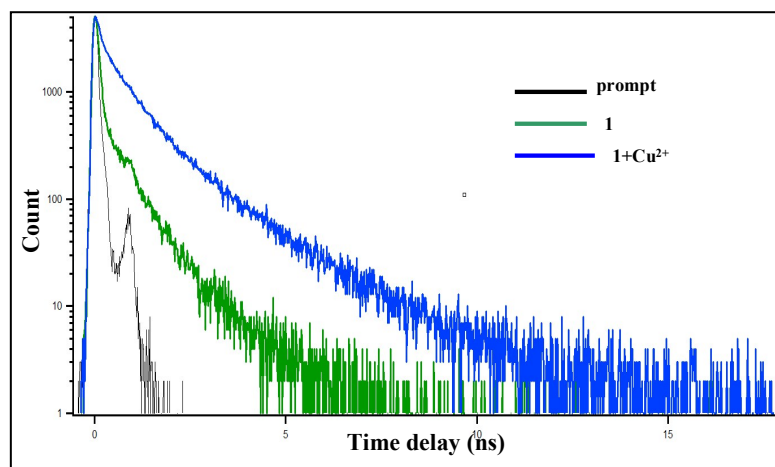


Fig. S13 Fluorescence decay profile of **1** and **1** in presence of 2 equivalents of Cu^{2+} , $\lambda_{\text{ex}} = 375 \text{ nm}$, $\lambda_{\text{em (max)}} = 570 \text{ nm}$

5. Theoretically optimized structure

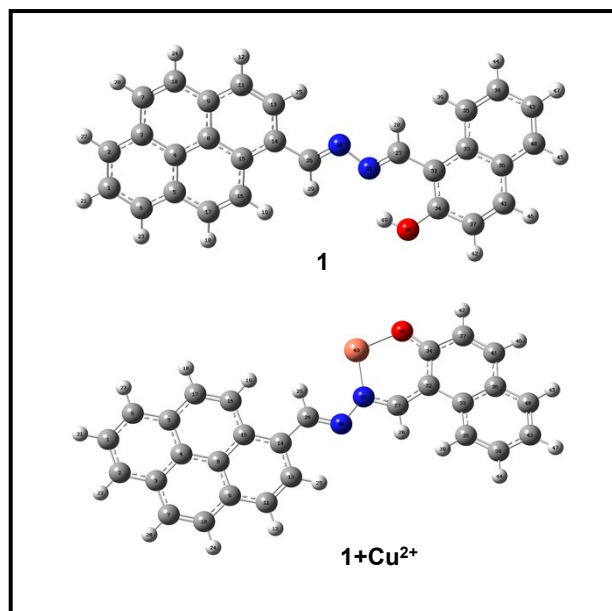


Fig. S14 Theoretically optimized structure of **1** and **1-Cu²⁺**

6. UV-Vis Spectral data of 1 with F⁻

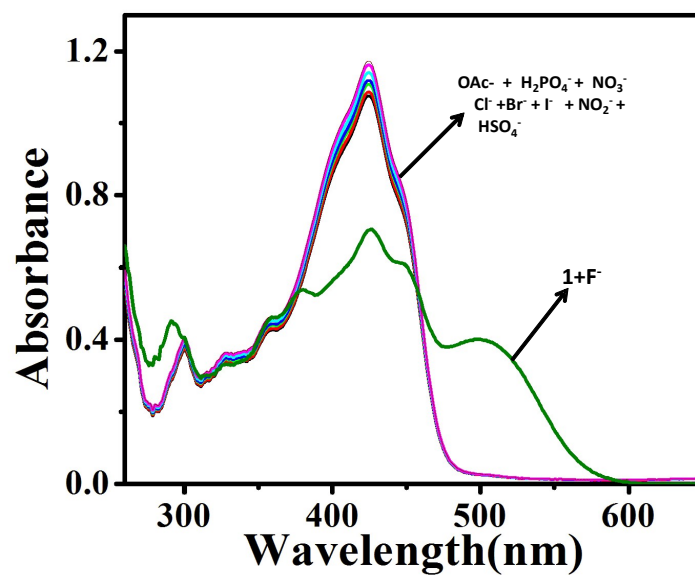


Fig. S15 UV-Vis spectral changes of sensor **1** (1×10^{-6} M) in presence of various anions (2 equiv.) in DMSO-water mixture (7:3, v/v)

7. ^1H NMR titration

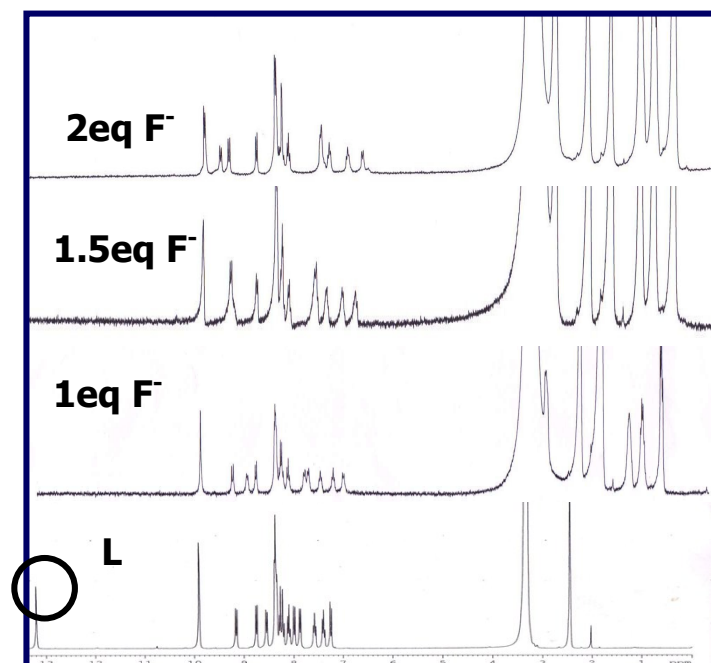


Fig. S16 ^1H NMR titration of **1** with tetrabutyl ammonium fluoride in $\text{DMSO-}d_6$

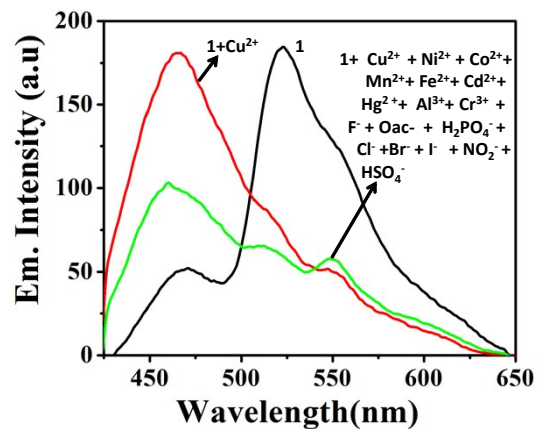
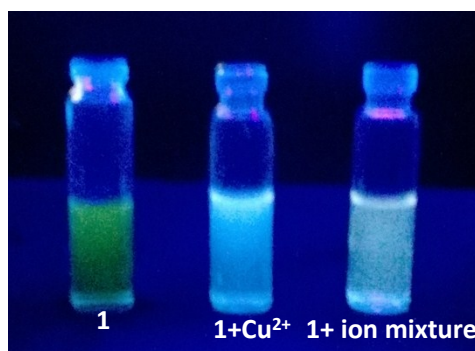


Fig. S17 Visual fluorescence change of **1** (1×10^{-5} M) (left) and fluorescence spectra of **1** (1×10^{-7} M) (right) in bare copper ion and in mixture of ions (Cu^{2+} , Ni^{2+} , Co^{2+} , Mn^{2+} , Fe^{2+} , Cd^{2+} , Hg^{2+} , Al^{3+} , Cr^{3+} , F^- , OAc^- , H_2PO_4^- , Cl^- , Br^- , I^- , NO_2^- and HSO_4^-) in methanol water mixture (7:3, v/v)

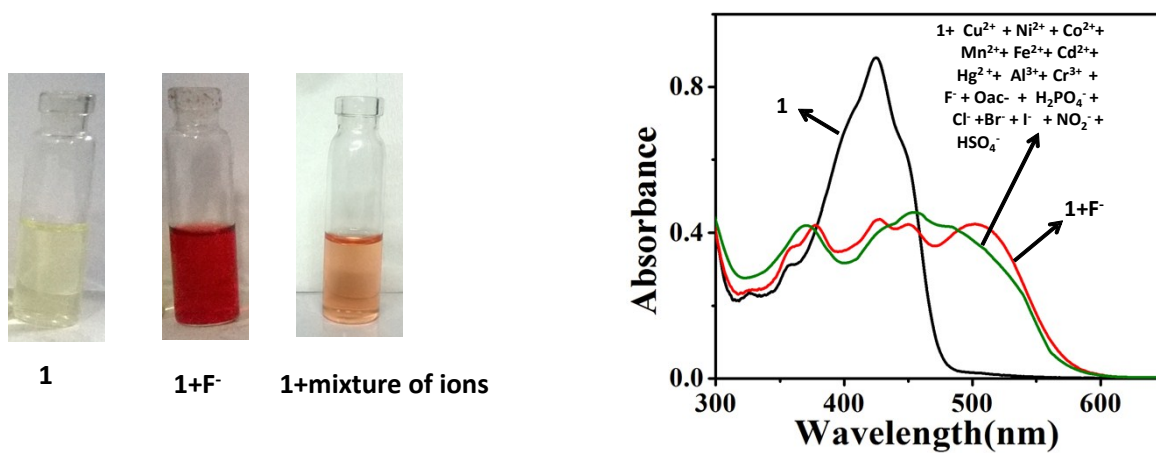


Fig. S18 Naked-eye color change of **1** (1×10^{-4} M) (left) and Uv-vis spectra of **1** (1×10^{-6} M) (right) in bare fluoride and in mixture of ions (Cu^{2+} , Ni^{2+} , Co^{2+} , Mn^{2+} , Fe^{2+} , Cd^{2+} , Hg^{2+} , Al^{3+} , Cr^{3+} , F^- , Oac^- , H_2PO_4^- , Cl^- , Br^- , I^- , NO_2^- and HSO_4^-) in DMSO water mixture (7:3, v/v)

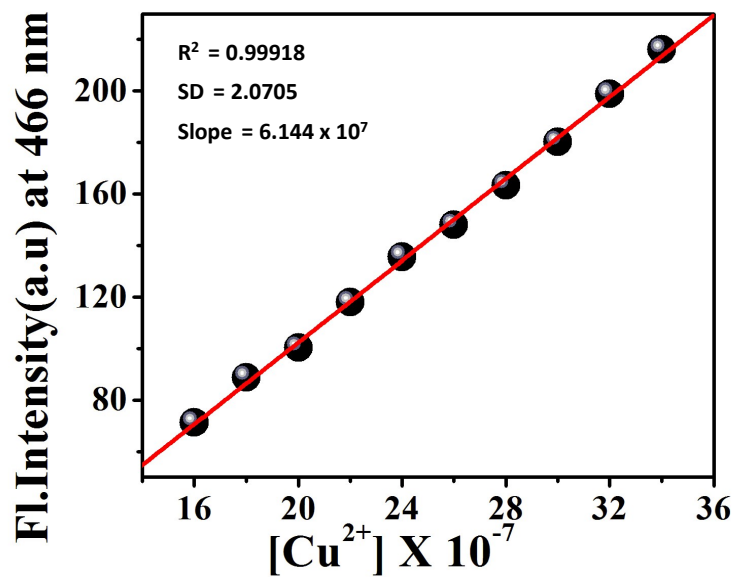


Fig.S19 Determination of detection limit of Cu^{2+} by **1**(1×10^{-7}) in methanol water mixture (7:3, v/v) at $\lambda_{em} = 466nm$.

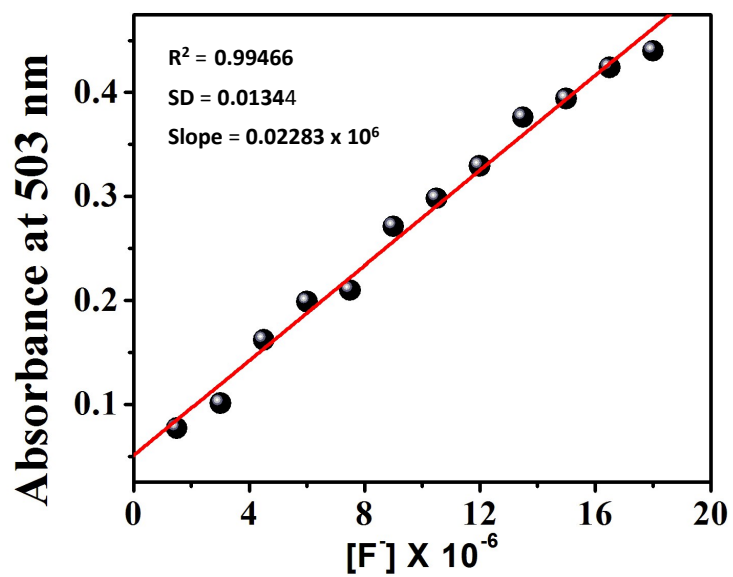


Fig. S20 Determination of detection limit of F⁻ by 1(1 × 10⁻⁶) in DMSO water mixture (7:3, v/v) at λ_{abs} = 503 nm.

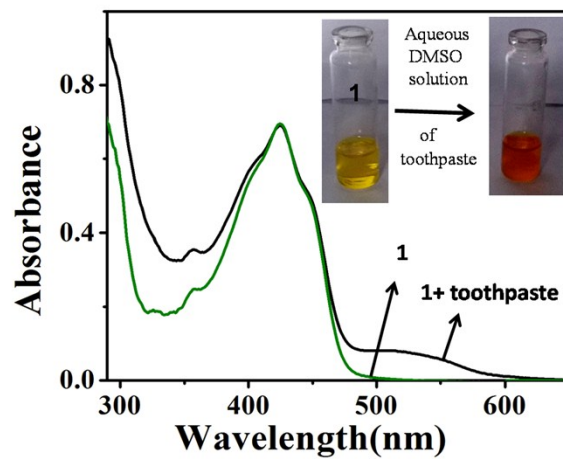
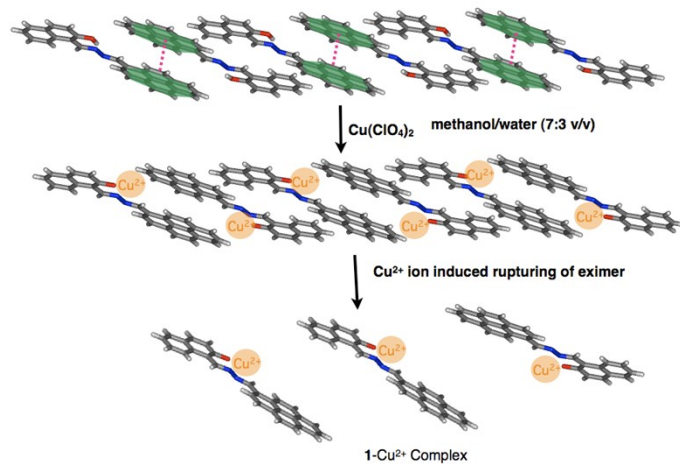
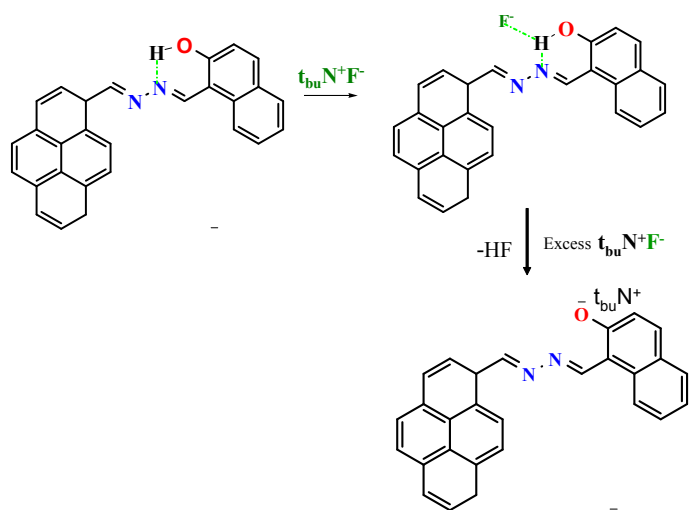


Fig. S21 Uv-vis spectra of **1** (1×10^{-5} M) and **1** in presence of toothpaste in aqueous DMSO solution and Naked-eye color change (inset).



Scheme S1. The plausible representation of the complexation of **1** with Cu^{2+}



Scheme S2. The plausible representation of the H-bonded form and the deprotonated form of receptor **1**.